

Trapping of fine-grained sediment on a supply-limited intertidal shore platform at Kaikōura, New Zealand

S.L. Horton^{a,b,*}, W.J. Stephenson^b, M.E. Dickson^c

^a School of Geography and the Environment, University of Oxford, Oxford, UK

^b School of Geography, University of Otago, Otago, New Zealand

^c School of the Environment, University of Auckland, Auckland, New Zealand

ARTICLE INFO

Keywords:

Shore platform
Suspended sediment
Time integrated mass-sediment sampler
Intertidal sediment trap

ABSTRACT

Shore platforms are generally supply-limited environments and few studies have attempted to measure sediment transport within this rock coast setting. This paper summarises a field-based pilot study that successfully collected fine-grain sediment moving across a sub-horizontal platform at Mudstone Bay, Kaikōura, New Zealand. Two large-aperture and two small-aperture Time-Integrated Mass-sediment Samplers (TIMS) were deployed for 9-days, encompassing 2 days of storm conditions (offshore significant wave heights between 2.0 and 3.6 m, with sediment trapped in both landward and seaward facing directions. The net flux of sediment captured in large aperture samplers was greatest in a seaward-direction (15.2 g), whereas the narrow-mouth samplers, that principally collected suspended sediment had a net onshore flux (5.4 g). The sediment traps yielded sufficient sample to undertake geochemical and textural analysis. Interpretation of these data suggests that the origin of transported material was autochthonous to the platform, being >80 % silt-sized and compositionally consistent with material derived from the shore platform and/or cliff colluvium. This pilot experiment demonstrates that mass-sediment samplers can be used in supply-limited intertidal shore platform settings. Further research involving greater sampling frequency and duration and concomitant detailed hydrodynamic measurements are likely to reveal important insights into the erosion environment.

1. Introduction

Sediment accumulations on shore platforms commonly occur at the base of cliffs as colluvium (Hall et al., 2008), as back beaches of storm deposits (Kirk, 1977; Kennedy and Milkins, 2015), or as cover deposits on low-lying Holocene marine terraces at the base of cliffs (Kennedy and Beban, 2005). The intertidal zone shore platforms are, however, mostly free of sediment build-up (Trenhaile, 2016), with the exception of boulder accumulations proximal to the astronomical high tide level (Chen et al., 2011; Etienne and Paris, 2010; Paris et al., 2011; Naylor et al., 2016), or deposition within platform runnels (Moses and Robinson, 2011; Moses, 2014). Sediment build-up may occur at the seaward edge of shore platforms, where sands or gravels bury the outer platform ledge below the low-tide elevation (Kennedy, 2015). Examples of seaward-edge accumulations have been reported in both macrotidal (e.g., Bay of Fundy, Canada, Porter et al., 2010) and microtidal (e.g., Shag Point, New Zealand, Kennedy and Dickson, 2006) environments. These sediment deposits at the seaward edge are likely ephemeral in response

to storm events (Kennedy and Milkins, 2015), but represent a source material that could to abrade shore platforms, or nourish beaches at the landward edge of otherwise bare platforms.

Where sand and coarse-grained sediment does occur on shore platforms, it may act as an abrasive agent to accelerate downwearing and notching of the cliff toe (Horikawa and Sunamura, 1970; Robinson, 1977; Kennedy and Beban, 2005; Blanco-Chao et al., 2007; Cullen and Bourke, 2018). Rock hardness is commonly used to describe the weathered state of shore platforms and has been used as a surrogate indicator for sediment abrasion. For example, Blanco-Chao et al. (2006, 2007) correlated an increase in rock hardness from rebound values (either Schmidt hammer or Equotip durometers) to parts of the shore platform that are regularly abraded. Thus, sediment abrasion may result in greater mechanical strength of the rock because it removes the weathered layer and thereby reduces roughness (Feal-Pérez et al., 2009; Feal-Pérez and Blanco-Chao, 2013), as well as impeding biological colonization (e.g., Naylor et al., 2012). As such, the movement of sediment over the intertidal zone may contribute to platform morphology,

* Corresponding author at: School of Geography and the Environment, University of Oxford, Oxford, UK.

E-mail address: sophie.horton@ouce.ox.ac.uk (S.L. Horton).

especially if it occurs at such rates as to abrade surfaces and cause surface denudation.

Previous studies on the movement of coarse clastic sediment on shore platforms shows that these environments have high transport potential but are generally supply-limited environments (Trenhaile, 2016). Platforms with an abundant sediment supply may lead to sediment accumulation that provides a protective cover that inhibits any further development of the shore platform profile. Where platforms are covered in boulders for example, presence of an armouring boulder layer may cause beach gradients increase with increasing grain size so that platform gradient in transport limited areas remains high (Pérez-Alberti et al., 2012). Conversely, in supply limited environments sediment-movement induced erosion may reduce bare platforms to gently sloping surfaces, consistent with tidal range and rock hardness (Pérez-Alberti et al., 2012). The concept of transport capacity in geomorphology was first introduced by Gilbert (1877, 1914), who noted that riverine systems will convey as much sediment as capacity allows (i.e., transport-limited), unless there is insufficient material to be transported (i.e., supply-limited). The concept of sediment-transport capacity appears to be used infrequently in coastal geomorphology compared to other environments (Wainwright et al., 2015), although it has been applied to longshore beach sediment transport, coastal engineering, and Bagnold's (1946; Bagnold, 1966) application of shear velocity and sediment movement (see: Wainwright et al., 2015). The concept is useful to shore platforms because depending on the environmental context they may be transport-limited environments (e.g., coarse clastic deposits like large boulders), or present as sediment-limited environments (e.g., bare platforms in the intertidal zones), subject to the interaction between material supply and flow competence.

Analysis of the movement of sediment transport on beaches, for example, has shown that sediment entrainment is controlled by bed shear stress, which is proportional to flow velocity (Masselink et al., 2005). In the swash zone, sediment movement occurs principally as bedload where individual grains are rolled or saltated along in sheet flow (Horn and Mason, 1994; Masselink and Puleo, 2006), although sediment will also be transported in suspension (Masselink et al., 2005). Hydrodynamic differences in turbulence from bore collapse (during uprush) or surface drag (during backwash) will preferentially affect sediment transport pathways, and whether conditions are more suitable to sheet flow or suspension in the swash zone (Masselink et al., 2005). Sediment transport on intertidal shore platforms, by comparison, is a highly dynamic process (McKenna et al., 2011; Naylor et al., 2016) where transport rates are controlled by material size and shape as well as platform topography and surface roughness (Nott, 2003).

Finer sediment (e.g., silt, sand and small pebbles) accumulations beyond the cliff toe to the seaward edge are rare due to limited sediment supply on shore platforms and because platform surfaces weather too slowly to form or sustain beaches (Trenhaile, 2005). This is also true for platforms comprising weakly lithified fine-grained sediments that erode quickly (e.g., siltstones, mudstones, or chalk) and yield fine-grained sediment but when denuded is easily transported offshore (Trenhaile, 2004). There have been no investigations to date that have observed fine-grained sediment transport on shore platforms and little is known about its textural composition, flux direction, or its capacity to contribute to the abrasion of platform surfaces.

Following co-seismic uplift of the Kaikōura Peninsula, New Zealand, in 2016, fine granular material began accumulating at the new supratidal cliff-toe of the shore platforms (Dickson et al., 2022). These deposits have several possible origins: remnant deposits from colluvium and co-seismic tsunami associated with the 2016 earthquake (see Power et al., 2017); in-situ accumulation of the sediment produced by platform downwearing, which are no longer swept away by regular tidal inundation; and/or storm deposits that sweep allochthonous material landward onto the shore platform. If the build-up of material is sustained by storms, this suggests that (1) during storms waves are able to inundate the supratidal zone (e.g., Horton et al., 2022a), (2) there is a sediment

source that can be entrained, and (3) wave conditions at the supratidal cliff-toe are conducive to sediment deposition. The post-uplift accumulation of suspended sediment at Kaikōura presents an opportunity to ascertain whether fine-grained material in transport can be collected, and whether its net flux can be determined. To assess whether these deposits are associated with storm-driven sediment transport, bespoke sediment samplers were designed and deployed for use on a shore platform at Mudstone Bay, Kaikōura. The objectives of this study are:

- 1) Trial the designs of time-integrated mass-sediment samplers (TIMS) to the novel setting of an intertidal shore platform that is exposed to bi-directional flow;
- 2) Resolve whether sediment traps yield sufficient sample mass to determine sediment provenance; and
- 3) Quantify the principal direction of sediment transport across the shore platform and its geomorphic significance at Kaikōura.

2. Study site

Te Taumanu o Te Waka a Māui/Kaikōura Peninsula is located on the east coast of Te Waipounamu/South Island of New Zealand (Fig. 1). The area has significant co-seismic uplift due to convergence along the Marlborough Fault System and proximity to the Hikurangi Subduction Zone (Howell and Clark, 2022). Long-term net uplift rates are estimated at 1.5 mm yr^{-1} with evidence of co-seismic faulting for at least 100 kys, with three Pleistocene-aged (ca. 123–55 ky BP) marine terraces (Ota et al., 1996; Duffy, 2020; Nicol et al., 2022). Discontinuous fragments of Holocene-aged co-seismic terraces are preserved around Kaikōura Peninsula ca. 850–550 and 350–100 years (McFadgen, 1987; Howell and Clark, 2022), with the most recent co-seismic uplift in 2016 forming an incipient marine terrace (Dickson et al., 2022; Nicol et al., 2022). Coastal subsidence of $1\text{--}3 \text{ mm yr}^{-1}$ occurs during interseismic periods due to the partial locking of the subducting crustal plate (Wallace et al., 2012), so that prior to the 2016 earthquake the coastal margins of Kaikōura were observed from the GNSS network to be subsiding (Nicol et al., 2022).

The contemporary Kaikōura Peninsula coastline has a series of projecting points and small bays with a near-continuous fringe of intertidal shore platforms (Fig. 1), presenting as both sheltered bay and exposed point platforms (Duckmanton, 1974; Kirk, 1975, 1977). The platforms of Kaikōura have been the site of a long monitoring experiment (since 1973) that has identified rapid downwearing rates attributed to sub-aerial weathering (e.g., Kirk, 1977; Stephenson and Kirk, 2000; Stephenson et al., 2017; Horton et al., 2022b; Omidiji et al., 2022). The Kaikōura coastline is microtidal, with average offshore significant wave heights (H_s) of $<2 \text{ m}$ typically from a southerly direction, although 31 % of waves originate due east producing small H_s swell waves $<0.8 \text{ m}$. Annual storms (with an occurrence 3–4 times a year) originate from the south where $H_s > 2 \text{ m}$ (Horton et al., 2022a). Wave conditions during the experimental period were characterised using data from WavewatchIII for the nearest cell to the Kaikōura Peninsula (42.5° S , 174° E).

Within this broader context, the study location for our experiment was Mudstone Bay, a sheltered sub-horizontal shore platform located on the southern side of Kaikōura Peninsula comprised of poorly bedded calcareous mudstone of the Waima Formation (Rattenbury et al., 2006) (Fig. 2a). The platform surface has a gentle slope (-0.59°), and a seaward edge demarcated by a low tide step ('Type B' platform). Co-seismic uplift vertically displaced the Mudstone Bay shore platform by $+0.95 \text{ m}$ (Horton et al., 2022c) so that its contemporary morphology has an intertidal width of approximately 50 m , and a supratidal incipient marine terrace of a similar width. The accumulation of material at the cliff toe (Fig. 2b) shows the accumulation of fine-grained sediment and organic detritus that has built up since the 2016 earthquake, and cliff erosion depositing fans of colluvium at the cliff toe-platform interface (Fig. 2c).

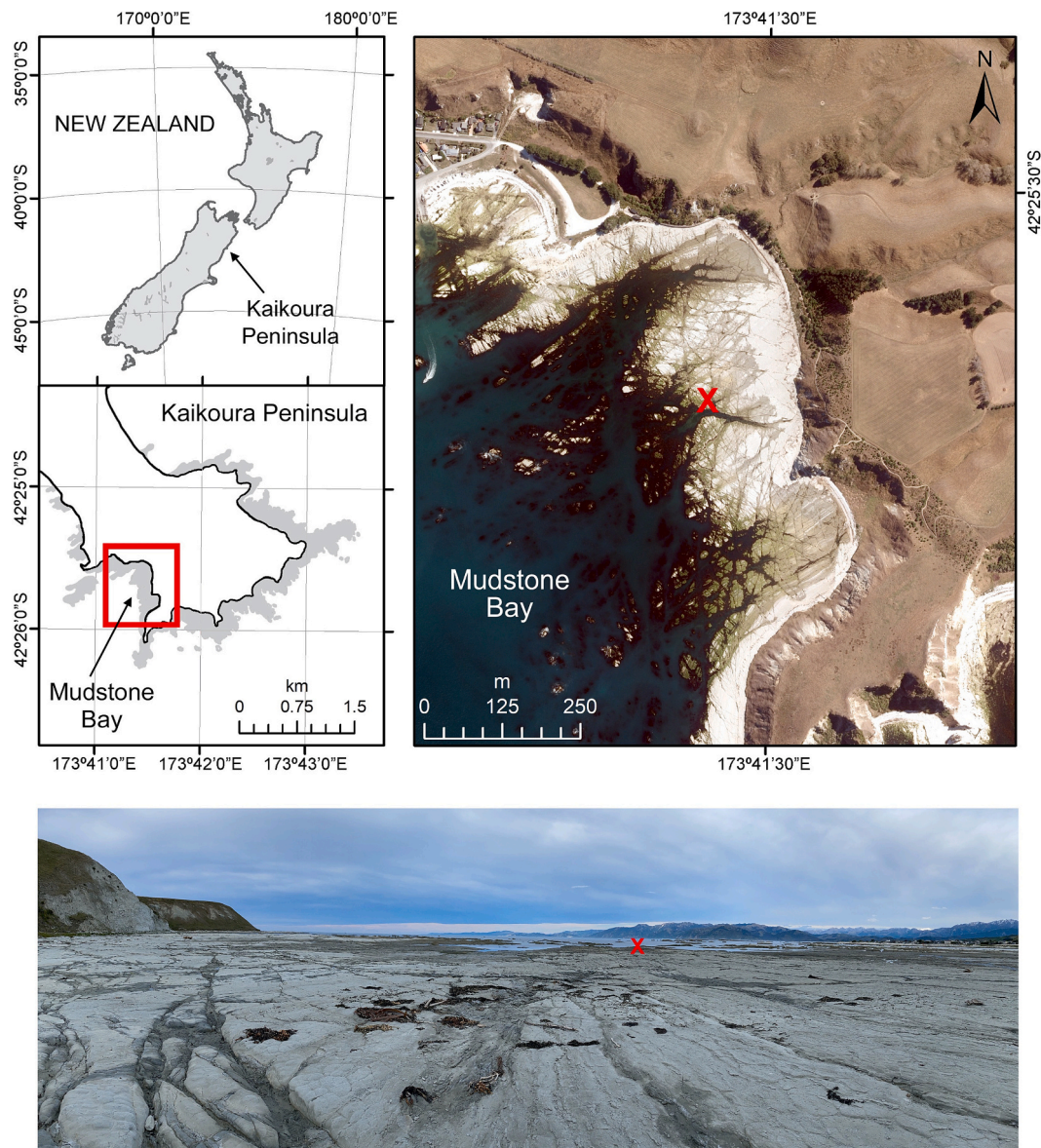


Fig. 1. Location of instrument deployment at Mudstone Bay, Kaikōura. The location of sediment traps is marked with an “X”. Photograph taken looking due south (179°S) approximately 56 m from the sediment traps.

3. Methods

3.1. Sediment trap design

To address the objectives of this study, it is pertinent to assess sediment trap design in the context of shore platforms and review existing sediment trapping techniques relevant to rock coasts. Sediment traps are used extensively in subtidal environments (e.g., vertical traps as reviewed by Butman, 1986), but rarely in estuarine or in intertidal environments due to the complexities of bi-directional flow. Vertical traps are seated within the substrate, with a wide mouth to height ratio ($> 3:1$) that promotes sediment settling in the subtidal zone when flow velocities $< 0.2 \text{ m s}^{-1}$ (Butman, 1986; White, 1990). Vertical traps are difficult to deploy in shallow intertidal zones since they are easily damaged by waves (Schiel et al., 2006). A “J-type” chamfered pipe (with a 15:1 ratio between pipe length and intake diameter) was shown by Schiel et al. (2006) to be an effective sediment trap in the intertidal zone of a shore platform. The medium-sized “J-type” traps were 820 mm long, with a 55 mm mouth and shown in laboratory experiments to retain between 75 and 100 % of coarse to fine silts for flow velocities $< 0.15 \text{ m}$

s^{-1} . The shortcoming of “J-type” traps is that they cannot account for directional flux of material in *bi-directional* flow, and likely overestimate net sediment flux by collecting material as it zig-zags across the intertidal zone due to oscillatory flow on both the rising and falling tide.

Time-integrated mass-sediment samplers (TIMS) are designed to continuously capture suspended sediment, in uni-directional flow environments (e.g., Phillips et al., 2000) or in bi-directional flow environments when two samplers are paired facing opposite directions (e.g., Elliott et al., 2017). Both operate on the principle that flow enters the sampler at its ambient velocity through a small aperture inflow tube (i. e., $< 4 \text{ mm}$). Flow expansion occurs inside the wider body of the sampler, causing a decrease in velocity and promoting sediment settling (Emmett, 1980). Water then exits the sampler through an outflow tube to allow for unimpeded flow. In a bi-directional flow environment, a chamfered outlet tube reduces internal turbulence and impedes sediment entry into the sampler during flow reversal (Elliott et al., 2017). TIMS are effective at retaining silt and clay fractions over a range of flow velocities (Elliott et al., 2017) and on this basis were selected for use on the shore platform.

Two sediment trap types were trialled in this study (Fig. 3): a small



Fig. 2. Photographs of Mudstone Bay, Kaikōura, showing the characteristics of the shore platform at low tide (a), the build-up of surficial deposits at the back of the platform (b), and cliff colluvium (c).

aperture trap based on the Price sampler designed to collect suspended sediment (Phillips et al., 2000; Elliott et al., 2017) and a large aperture trap based on a Helley-Smith sampler designed to capture creeping, saltating, and rolling sediment (Emmett, 1980). Unlike the Helley-Smith design, which has a mesh body, the large aperture TIMS used in this study have a solid PVC body that may also trap fine sediment in suspension. The small aperture sampler was made from pressure grade PVC piping fitted with a 4 mm internal diameter (ID) intake. The ID tube body was 45 mm, yielding a trap-to-intake ratio of 11:1. The sampler tubes were 1000 mm in length, yielding a trap collection volume of 1590 cm³.

Previous efforts at partitioning bedload and suspended load in beach studies have generally considered heights above the bed >0.1 m to be in suspension (Horn and Mason, 1994), but these are related to the pragmatics of trap design rather than the physics of keeping particulates aloft (Hughes et al., 1997). Other studies have estimated suspended sediment concentration as being a nominal fixed height above the bed (e.g., 30 mm) and monitored using optical back scattering instruments (e.g., Austin and Masselink, 2008). So, within coastal applications there is no fixed height above the bed that is considered standard for the capture of suspended sediment. The small aperture TIMS intakes are purposely above the bed, usually 0.1–0.2 m above a riverbed for suspended sediment sampling (Phillips et al., 2000). When deployed in the tidal estuarine environment by Elliott et al. (2017), the bi-directional TIMS were mounted 0.5 m above the seabed. By seating the sampler above the bed-level these samplers are above any saltating load (or creeping sheetflow)

and less likely to be inundated by sand or gravel movement, or invaded by benthic fauna. However, the location of the intake nozzle relative to total water depth will affect the sampling efficiency of the sampler, since sediment concentration is not uniformly distributed through water depth, but rather the greatest sediment concentration is associated with bottom waters compared to surface waters in the nearshore zone (Kirk, 1971; Shetty et al., 2022), akin to its distribution in fluvial environments with bed-shear parameterised using Shield's parameter (Masselink et al., 2005; Masselink and Puleo, 2006).

The large aperture sediment traps are designed to collect rolling and saltating material close to the bed surface ('bedload') and fitted with a semi-circular 740 mm² intake with a rubber uni-directional baffle to allow easy fluid ingress into the tube and reduce backflow loss out of the large sampler mouth (Fig. 3). The sampler mouth is a reducing rectangular scoop that tapers into a semi-circular intake. The sampler body is made from PVC piping with an ID tube body of an 85 mm and 500 mm length, yielding a trap collection volume of 2837 cm³. Each trap had a 90° chamfered outlet pipe with an ID of 20 mm. The intake of the large aperture samplers was approximately 1:2 of the sampler tube, and slightly less than the 1:3 specified in the original Helley-Smith sediment samplers (Emmett, 1980), which may reduce effective sedimentation inside the sampler body. To promote sedimentation inside the sampler body a forward baffle was installed to reduce counter flows on the tidal ebb, and a rear mesh baffle to reduce turbulence and backpressures.

Both traps (small and large aperture) had an internal fine mesh baffle at the rear of the pipe to reduce any fine grain sediment loss or turbulent

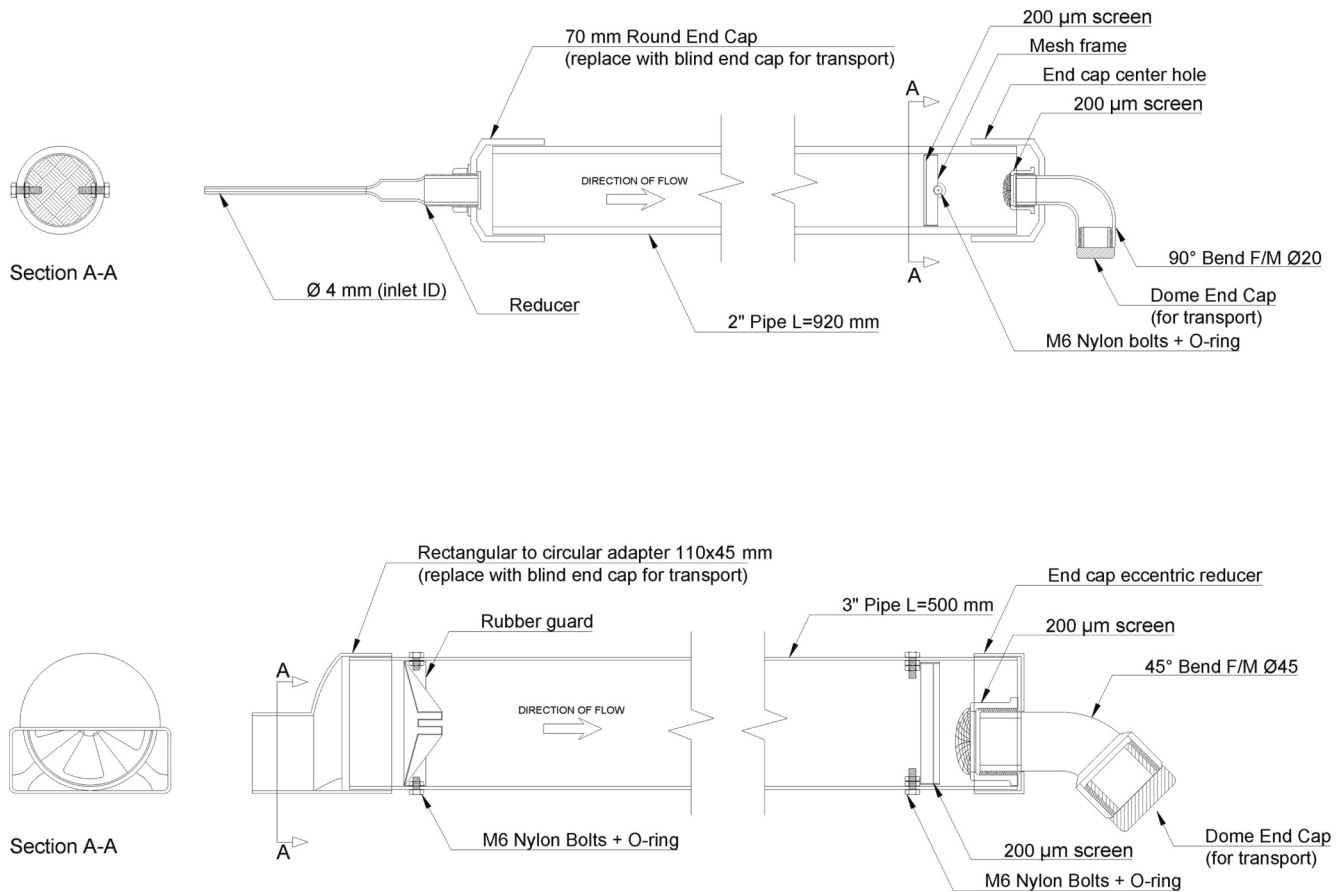


Fig. 3. (Top) Technical schematic of small aperture suspended sediment time-integrated mass-sediment sampler, based on design of Price samplers; (bottom) technical schematic of wide aperture bedload sediment time-integrated mass-sediment sampler based on design of Helley-Smith samplers.

backpressure within the pipe (Fig. 3). The traps were deployed as a pair, with one facing landward, and the other facing seaward. Sediment traps were secured to the bed surface using metal straps into pre-drilled stainless steel mounting plates that were bolted into the shore platform. At the conclusion of the deployment each end was securely capped and transferred to a laboratory where the sediment was washed out using distilled de-ionised water.

3.2. Instrument deployment and in situ measurements

Two sets of paired sediment traps were deployed at Mudstone Bay and left to accumulate material for 9 days (24 September to 2 October 2020). Each trap pair comprised one seaward-facing trap and one landward-facing trap (Fig. 4). Samplers were bolted to the platform and secured with metal plates. Two RBR Duet pressure transducers were installed, one at the seaward edge, and the other between the intakes of the seaward-facing sediment traps (Fig. 5). Pressure transducers recorded continuously at 2 Hz. Data were barometrically adjusted and processed to obtain water depth and spectral frequency (see: Horton et al., 2022a).

Surface hardness of the shore platform was assessed at six locations (Fig. 5) using a Proceq Equotip 550 with a Leeb hardness method type D (HLD). The hardness measurements were included in the study to ascertain whether there was any surficial evidence of surface abrasion that could be attributable to sediment transport across the platform. The Equotip measures in situ impact and rebound velocities, which are proportional to material surface hardness (Viles et al., 2011; Coombes et al., 2013). Mean hardness values at each site were calculated from ten replicate measurements. Measurements were taken either side of a storm event, when sediment transport was most likely to occur, with

observations collected on 25 September 2020 (pre-storm) and 3 October 2020 (post-storm), with additional measurements taken the following year (October 2021 and December 2021) providing data unrelated to specific storm events. The surface was lightly brushed to remove any loose dust prior to hardness measurements to estimate the 'weathered' platform surface. An additional set of measurements were taken in October 2020 to determine the 'unweathered' rock hardness by removing a 5–10 mm layer of platform surface with a chisel to expose a smooth fresh rock surface.

3.3. Sediment treatment and analysis

The trapped sediment was washed from the collectors using distilled de-ionised water into 10 L containers and left for 7 days to settle, which was the time needed using Stoke's Law to settle clay-sized ($>1 \mu\text{m}$) particles (Ferguson and Church, 2004; Bright et al., 2018). Samples were desalted by repeated dilution and rinses of the retentate with distilled de-ionised water, ensuring not to disturb any of the settled sediment (Minor et al., 2014; Ayeku et al., 2021). The desalting was repeated until the retentate reached an electrical conductance $<100 \mu\text{S cm}^{-1}$ (i.e., salinity $<0.05 \%$, Gee, 2002) and any loose or floating organic material was removed during rinsing. The retained sediment was oven-dried at 40°C for 7 days and weighed using a 3-point decimal balance. A portion of the sediment samples was mounted and carbon coated for Scanning Electron Microscopy (SEM) using a JEOL FE-SEM 6700 to provide textural analysis of the sediment and analysed with Energy-Dispersive X-ray Spectroscopy (EDS) for detecting elemental composition of point-locations.

For particle size analysis 200 mg of sample was pre-treated with 30 % H_2O_2 and digested at 50°C for 24 h (Gee, 2002), or until all organic



Fig. 4. Bi-directional deployment of sediment traps on Kaikōura Peninsula at South Bay. Pressure transducer installed between the sediment traps inside metal casing.

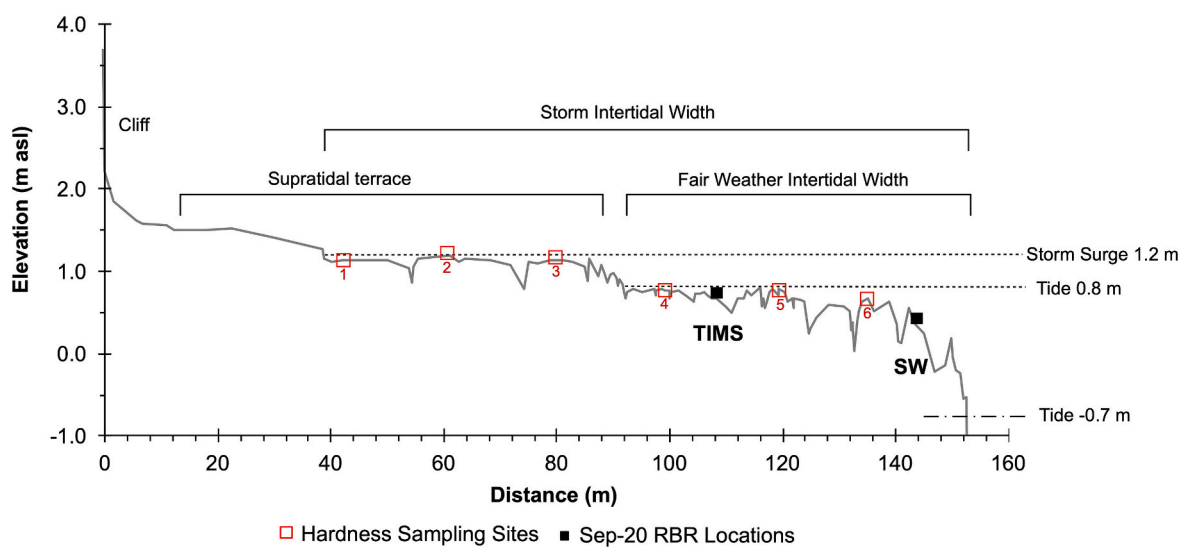


Fig. 5. Shore normal transect at Mudstone Bay showing relative deployment locations of the sediment traps (at TMS) and the two pressure transducers, one near the seaward edge (SW) and the other midway through the fair-weather intertidal zone of the shore platform. The tidal range during the sediment trapping experiment ranged from -0.7 to $+0.8$ m asl as indicated by the horizontal dashed line.

carbon had been chemically decomposed to CO_2 . Samples were centrifuged at 3000 rpm for 10 min to separate the supernatant from the sample. Samples were rinsed and centrifuged twice to remove the H_2O_2 reagent. To impede flocculation, 5 mL of $\text{Na}_6[(\text{PO}_3)_6]$ was added to the sample and agitated for 2 h (Gee, 2002). Samples were left to stand for 24 h and re-suspended using a vortex mixer. Particle size was measured using a Malvern 3000 laser particle size analyser with a Hydro2000 wet dispersal unit. Analysis of each aliquot was completed in triplicate, and the average particle size reported.

Geochemical analysis used portable X-ray fluorescence (pXRF) to determine the major oxides and trace metals. A DP-6000 Olympus pXRF was used in *geochem* mode and calibrated with two National Institute of Standards and Technology (NIST) soil samples (NIST 2710 A–I and NIST 2711 A–II). The pXRF cannot detect Na or Mg, however, these are minor constituents of the marl and limestone around Kaikōura Peninsula and contribute <2 wt% (weight percent) of the total oxides (Morris, 1987).

The analysis output is recorded in parts-per million (ppm) unit notation, which was normalized to a wt% for the major constituents. Trace elements are reported in ppm.

4. Results

4.1. Wave conditions

During the deployment, tides were transitioning to neap conditions. Tide 1 on the evening of the 24 September 2020 had a peak high tide of 0.8 m asl, but this decreased to a peak high tide height of 0.5 m by 2 October 2020 (Fig. 6). Offshore significant wave heights (H_s) were < 1 m between 24 and 26 September, then increased to 1.8 m on 27 September. Storm conditions occurred on 29 September when offshore significant wave heights exceeded 2 m and peaked at 3.6 m. The storm coincided with neap tides so that there is only a modest increase in water level

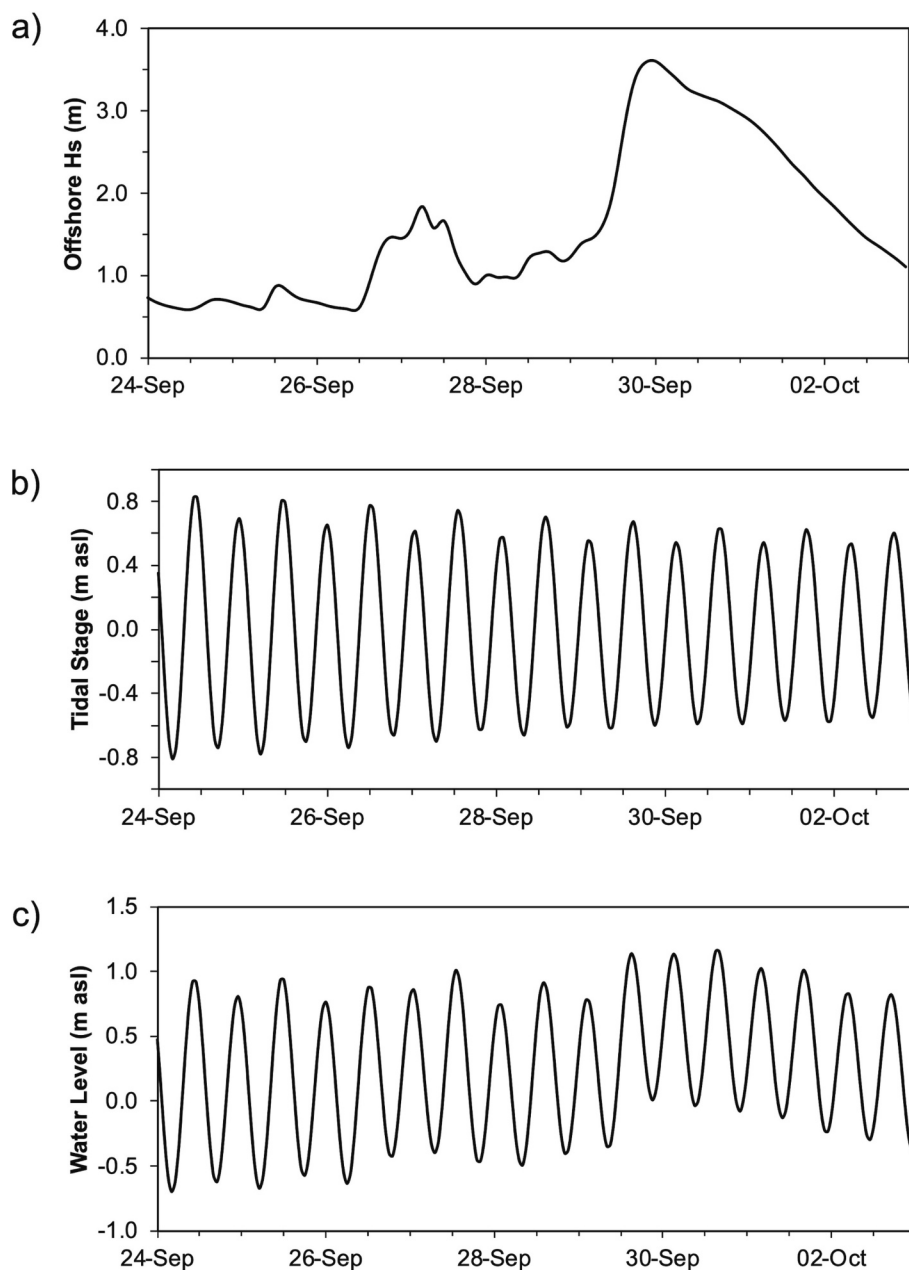


Fig. 6. Offshore wave conditions showing a) significant offshore wave height (H_s) as predicted by WaveWatchIII b) tidal stage (as m asl), and c) water level as predicted using an inundation calculation (in m asl, LVD-37).

across the platform, but this was sufficient to overtop and laterally inundate up to 50 m of the supratidal terrace (Fig. 5). Organic storm detritus was washed onto the supratidal zone (Fig. 2b).

4.2. Onshore wave conditions

During quiescent offshore conditions (tides 1–11) the shore platform at Mudstone Bay received very low wave energy ($< 1 \text{ J m}^{-2}$) at both the seaward edge and the sensor located next to the TIMS (Table 1). The wave spectra were 30–37 % infragravity energy, and there was little difference in significant onshore infragravity (H_{mOL}) and gravity (H_{mOH}) wave heights (0.06–0.10 m for both spectra at both sensor locations). The storm occurred on tides 11–13 arriving at Kaikōura on the 29–30 September where there was a 7-fold increase in measured total energy onshore, with a high tide mean of 5.1 J m^{-2} at the TIMS sensor and 7.05 J m^{-2} at the seaward edge sensor (Table 1). Under these storm conditions there was a significant increase in infragravity energy, contributing 55 % of total energy at the seaward edge and 76 % at the TIMS sensor (and sediment traps). There was a 4-fold increase in H_{mOL} to 0.24 m at both pressure sensors (Fig. 7). H_{mOH} increased substantially to 0.22 m at the seaward edge during the storm, but this effect was not translated to the sensor at the TIMS location notwithstanding a modest increase compared to the pre- and post-storm conditions where H_{mOH} was 0.13 m. These data suggest significant attenuation of gravity waves occurs between the seaward edge and the TIMS location. Post storm (tides 14–15) infragravity energy remained elevated and contributed most of the total energy (77 % at the seaward edge, and 92 % at the TIMS) (Fig. 7). Infragravity energy remained high post-storm at the TIMS sensor and did not return to its pre-storm levels within the experimental period, despite total energy decreasing to 0.44 J m^{-2} for tides 17–18.

4.3. Sediment flux

The large aperture TIMS were checked on the 26 September 2020 and a small amount of fine-grained sediment had accumulated in the pipes under quiescent wave conditions (Fig. 8a). The TIMS were collected on the 3 October 2020. On collection it was noted that a piece of rock had wedged under the nozzle intake of the seaward-facing small aperture TIMS (Fig. 8b). As expected, the large aperture TIMS trapped significantly more material than the small aperture samplers, with a net seaward flux of 15.2 g. By comparison, the small aperture TIMS collected the greatest load of material within the seaward-facing TIMS with 7.9 g, and only 2.5 g were collected from the landward-facing small aperture TIMS. Thus, the two sets of samplers had contradictory net fluxes of sediment movement, with the large aperture TIMS suggesting a net seaward flux of rolling and saltating material, and the small aperture TIMS had a net landward sediment flux of suspended material (Fig. 9).

4.4. Sediment composition, texture, and size

The pilot study was successful in that sufficient material was collected by the large aperture traps for physical and geochemical

analysis of the sediment transported across the platform. Silicates (SiO_2) dominated the sediment geochemistry ($\sim 50 \text{ wt\%}$), followed by calcium carbonate ($\text{CaCO}_3 \sim 30 \text{ wt\%}$), aluminium oxide ($\text{Al}_2\text{O}_3 \sim 9 \text{ wt\%}$), and iron oxides ($\text{FeO}^T \sim 4 \text{ \%}$) (Table 2). Few trace constituents were detected by the pXRF analysis, principally Sr, Br and Rb, which are representative of argillite basement rocks in New Zealand. There was no apparent difference in the geochemistry between the seaward-facing and landward-facing sediment traps and the sample of platform rock, implying that the sediment represents autochthonous material derived from the shore platform.

The sediment collected on the Kaikōura shore platform during the September – October 2020 sampling period was composed of poorly sorted silts, with a leptokurtic and strongly fine skewed particle distribution (Fig. 10). The small aperture TIMS had a dominant size mode peaking between 5.2 and 5.4ϕ ($23\text{--}26 \mu\text{m}$), whereas the large aperture TIMS were slightly coarser, with a peak mode between 4.5 and 4.9ϕ ($32\text{--}45 \mu\text{m}$). There was no difference between the particle size class distribution of the seaward- and landward-facing small aperture TIMS, but the landward-facing large aperture TIMS (that is, the flux of material was moving seaward and away from the cliff) had slightly coarser sediments, with the dominant mode at 4.5ϕ ($32 \mu\text{m}$) compared to the small aperture TIMS (Fig. 10). Based on the particle size distributions all samplers mostly collected silts (82–84 %), where clay contributed only 8–10 % and sand 4–8 %.

Examination of the washed and dried sediment samples under SEM showed that the grains were comprised of smooth surfaces of aluminium silicates, which presented either as smooth blocks (e.g., Fig. 11d) or as platy phyllosilicates (Fig. 11c). Aggregates containing calcium carbonate were also detected and tended to be irregular and rough. Fragments of biogenic material were present within aggregates, including algae and diatoms. The entrained sediments were irregularly shaped suggesting a short transport pathway and only one obviously polished grain was detected (Fig. 11a). The well-rounded grain in Fig. 11a is sand-sized and provides high textural contrast to the irregular siltstone.

4.5. Platform hardness

Platform hardness at Mudstone Bay showed little variation between pre- and post- storm conditions in September and October 2020. The supratidal stations (1–3) had a mean hardness of $315 \pm 34 \text{ HLD}$ pre-storm and $305 \pm 30 \text{ HLD}$ post-storm (Fig. 12). There was no significant difference within the 95 % confidence intervals (one-way ANOVA, $p > 0.05$) between the intertidal stations (4–6) hardness pre- ($316 \pm 34 \text{ HLD}$) and post-storm ($339 \pm 31 \text{ HLD}$) (Fig. 12). Measurements taken under quiescent conditions the following year in October 2021 and December 2021 showed that the pre- and post- storm hardness measurements were generally consistent with the weathered current platform hardness (overall mean 316 HLD). Assessment of the ‘unweathered’ platform showed that rock hardness by physically removing the weathered surficial layers was relatively consistent across the sampling stations with a mean of 397 HLD . Of these, the seaward edge (station 6) had a mean weathered surface of 284 HLD and was the

Table 1

Mean onshore wave conditions for the high tide period (2.5 h). Each tide contains 15 10-min bursts at the TIMS and SW (seaward) sensor locations.

Tide cycle	Depth (h)	H_{mOH}	H_{mOL}	TE (J m^{-2})	E_{IG} (%)	E_{SW}	E_{IG}	E_{WW}	H_{mOL}/H_{mOH}
TIMS									
1–11	0.28	0.08	0.06	0.75	37.0	0.30	0.27	0.16	0.79
12–14	0.23	0.13	0.24	5.08	75.8	0.77	3.92	0.35	1.85
15–16	0.09	0.06	0.19	2.78	91.8	0.15	2.56	0.07	3.40
17–18	0.02	0.02	0.07	0.44	92.1	0.02	0.42	0.01	4.48
SW									
5–11	0.34	0.01	0.06	0.91	30.3	0.23	0.29	0.35	0.67
12–14	0.29	0.22	0.24	7.05	54.6	2.06	3.89	0.99	1.11
15–16	0.14	0.12	0.22	4.20	76.8	0.56	3.26	0.34	1.83
17–18	0.06	0.05	0.08	0.71	64.4	0.11	0.50	0.09	1.38

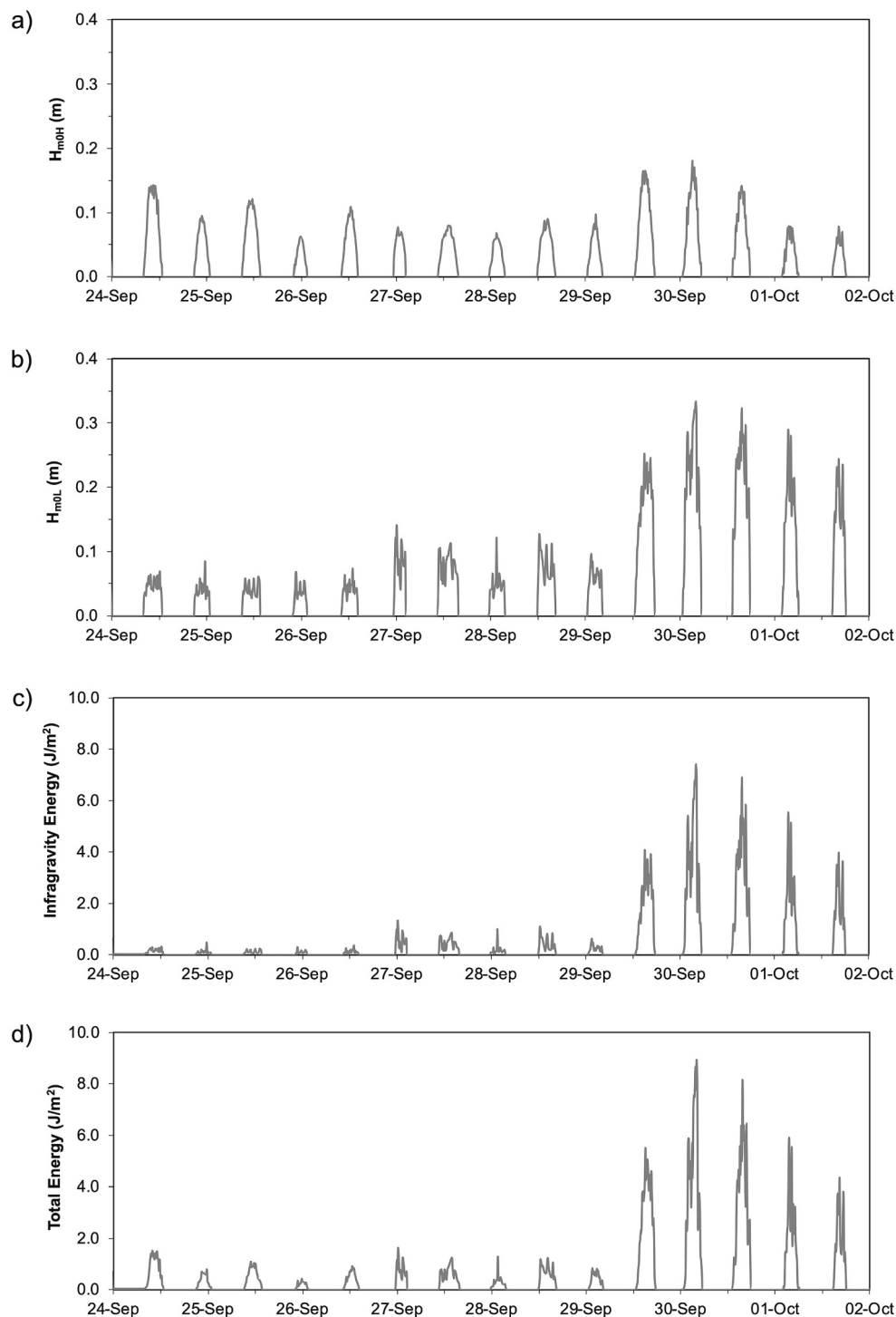


Fig. 7. Onshore wave conditions recorded at the seaward edge (SW) sensor for a) H_{m0H} , b) H_{m0L} , c) infragravity energy and d) total energy as recorded at Mudstone Bay between 24 September 2020 and 02 October 2020.

location of the weakest weathered surface, which may in part reflect sampling difficulty due to algal cover and/or higher rock moisture due to less drying time between tides. The hardness of the upper supratidal zone (stations 1 and 2) was 290 and 292 HLD, respectively, and associated with significant surface disaggregation through visible slaking.

5. Discussion

5.1. Assessment of sediment traps for intertidal shore platforms

Simple non-directional sediment traps have been previously used on the rock coast of Kaikōura Peninsula (Schiel et al., 2006). In their study, medium sized 'J' sediment traps collected <1 to 8 g of sediment per day, however, these fluxes cannot be directly compared to this study due to different trap design and the subsequent uplift of the shore platforms in 2016. Schiel et al. (2006) noted a similar range in particle-sized material



Fig. 8. a) Internal view of large aperture TIMS (26 September) after 2 days of deployment in quiescent conditions showing small amounts of fine-grained sediment accumulation. b) seaward-facing small aperture TIMS showing a clast wedged under intake following storm conditions that occurred between 29 and 30 September 2020.

as collected by the TIMS, and that sediment transport at Kaikōura contained very little sand. The deployment of TIMS in this pilot study flow velocity was not measured concurrent with the sediment collection, and further research is needed to ascertain any relationship between the sediment volume captured and sediment transport rates, and how these relate to flow velocities. Such work was outside of the scope of this study, but should be pursued as an avenue for further research.

In this pilot study the small-aperture intake nozzles were approximately 0.05 m above the platform surface and during the experimental period, tides were approaching neap, with mean high tide water depth (h) falling from 0.29 m (pre-storm) to 0.09 m (post-storm) reaching the TIMS. Consequently, during the neap tides the intake nozzle was 40 % of depth from the water surface, and too high relative to water depth to sample the depth of maximum suspended sediment. During the pre-storm and storm conditions, where water depth was 0.23 to 0.29 m, the nozzle depth was 78–83 % of water depth and well positioned to sample suspended sediment. It must also be noted, however, that Mudstone Bay receives low wave energy under quiescent conditions ($< 1 \text{ J m}^{-2}$), and the combination of low wave energy and no allochthonous supply of clastic sediment meant that relatively little suspended sediment was likely mobilised under quiescent conditions between the 24–28 September 2020. We infer that most of the trapped suspended material was likely mobilised during the storm of the 29–30 September 2020. In this regard, the height of the small-aperture TIMS intake nozzle may be a source of significant under-catch of entrained material relative to the large-aperture TIMS.

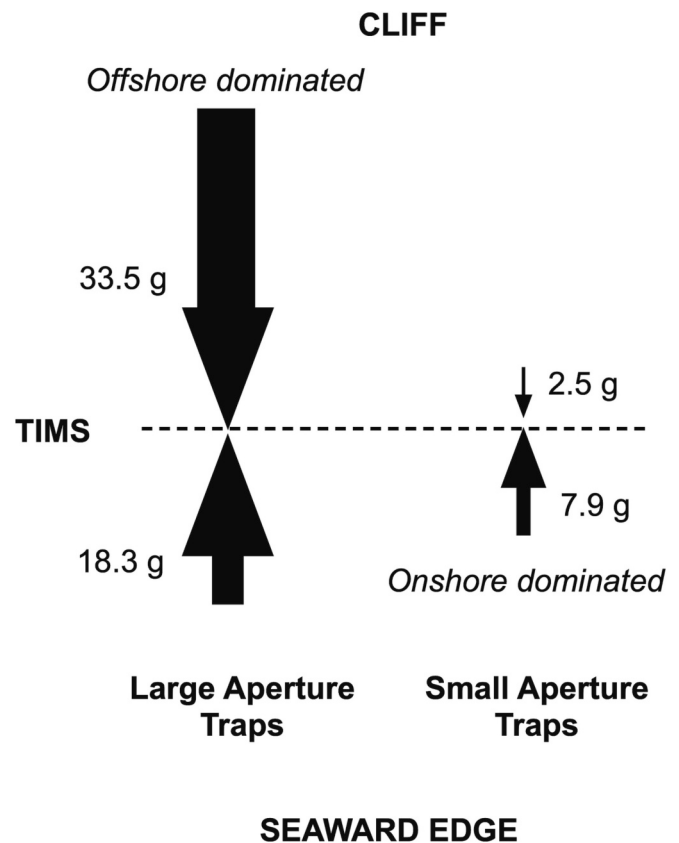


Fig. 9. Sediment mass captured over 9 days at Mudstone Bay, Kaikōura Peninsula using two different TIMS designs.

The large aperture TIMS collected up to 10 times more material than the small aperture TIMS. The large aperture TIMS also trapped small amounts of material prior to the storm (Fig. 8a), suggesting that 1) the large aperture TIMS are collecting suspended sediment under quiescent conditions and 2) are effective at collecting saltating sediment in the intertidal zone under storm conditions. The incongruity in net sediment flux between the two designs of TIMS deployed in this study probably reflects the capability of each sampler to vertically integrate entrained sediment, and how much material is transported relative to vertical velocity distribution in the water column (Fig. 13). The large aperture TIMS are open to a 0.05 m water column, compared to the 0.004 m intake of the small aperture TIMS that are only capable of sampling suspended sediment (Fig. 13), which in the context of beaches is held aloft due to turbulence induced from bore collapse associated with the seaward edge (e.g., Masselink and Puleo, 2006). The large aperture sampler mouth was no > 0.01 m above the bed, but due to the uneven platform surface could not be positioned fully against the bed, so some bedload possibly rolled underneath the intake, resulting in under-catch.

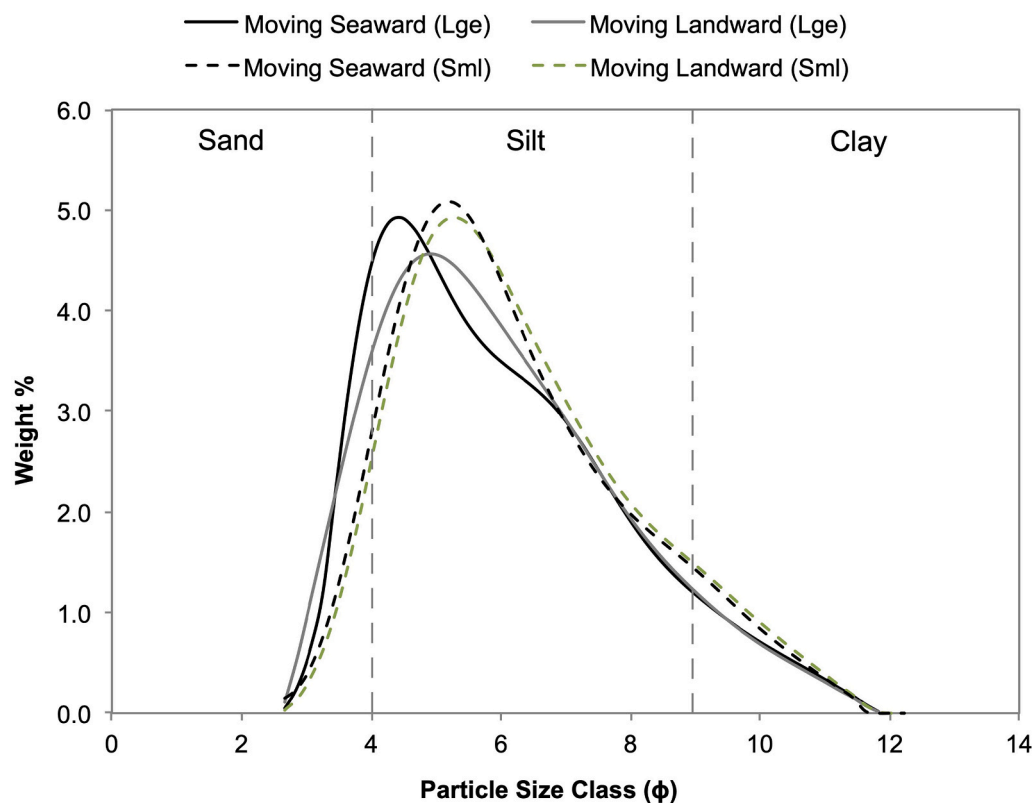
If it is assumed that the material trapped in the large aperture TIMS is generally representative of net sediment transport on the platform studied, then there was an overall net loss of sediment from the platform offshore. These results are consistent with the interpretation that, for a bare shore platform with little to no sediment accumulation, material lost via downwearing of the platform is swept offshore below the low tide cliff (Trenhaile, 2005; Trenhaile, 2016). In this regard, any autochthonous fine-grained sediment is unlikely to be stored as storm swash deposits because it breaks down into silt-grade material that is easily transported offshore. It is possible that runnels or topographic depressions may trap both swash and backwash transported material and abrade these localised areas (Dornbusch et al., 2007; Moses and Robinson, 2011), and there is evidence of fine-grained sediment, detached seaweed and small blocks of platform accumulating in the

Table 2

Geochemistry of mobilised sediment captured in the large aperture TIMS during the October storm.

Major oxides (wt%)	SiO ₂	Al ₂ O ₃	FeO	CaCO ₃	K ₂ O	TiO ₂	MnO	P ₂ O ₅	SO ₃
Platform Rock	41.1	11.1	4.4	39.5	2.2	0.7	0.1	0.0	0.7
Colluvium	36.2	6.9	3.7	50.2	1.4	0.6	0.5	0.0	0.7
Cover Deposit	47.6	9.6	5.6	27.0	2.5	0.3	0.0	0.0	1.6
TIMS Landward	51.3	10.0	4.4	29.0	2.2	0.3	0.1	0.0	0.7
TIMS Seaward	47.6	8.9	4.4	32.9	2.4	0.2	0.0	0.0	1.6

Trace (ppm)	Ba	Nb	Rb	Sr	Y	Zn	Zr
Platform Rock	499	11	83	559	10	109	131
Colluvium	530	11	97	557	11	89	127
Cover Deposit	563	8	81	642	16	77	130
TIMS Landward	544	10	105	609	16	152	173
TIMS Seaward	489	9	124	657	10	163	130

**Fig. 10.** Particle size distribution ($\phi = -\log_2 \text{mm}$) for sediment caught in sediment traps on the Kaikōura Peninsula.

runnels that bisect the platform at Mudstone Bay. Despite evidence of sediment transport during storms at Mudstone Bay, there was no observable effect on platform hardness.

5.2. Provenance of sediment transported on the mudstone bay shore platform

Sediment collection on the sub-horizontal shore platform at Mudstone Bay, Kaikōura, has shown that it is possible to discern sediment movement across a shore platform using TIMS. The size of material transported as either bedload or suspended load was dominated by silt (20–40 μm), which is easily transported under the hydrodynamic conditions observed (i.e., is not transport-limited) and consistent with material eroded from the siltstone/mudstone shore platforms. There was little difference in the particle size distributions collected between the small and large aperture traps suggesting that both collected representative samples of the material being transported, and generally agrees with observations of previous use of TIMS (Elliott et al., 2017; McDonald

et al., 2010; Perks et al., 2013).

The provenance of the transported material could not be geochemically distinguished between shore platform bedrock, cliff aggregate, back beach accumulation, and the sediment caught in the TIMS (both saltating and suspended). This is indicative of an autochthonously derived supply-limited environment. Textural analysis using SEM imagery showed fragments of marine organic matter caught in the wide aperture TIMS, which likely reflects material disturbed from algae colonies on the seaward region of the shore platform. In this regard, it is likely that sediment being trapped on the shore platform is at least in part derived from the weathered shore platform surface. Under storm conditions, however, significant fragments of organic matter will likely be held aloft in the water column and this will also wash algal fragments into the landward-facing samplers (i.e., moving in a seaward direction) through backwash.

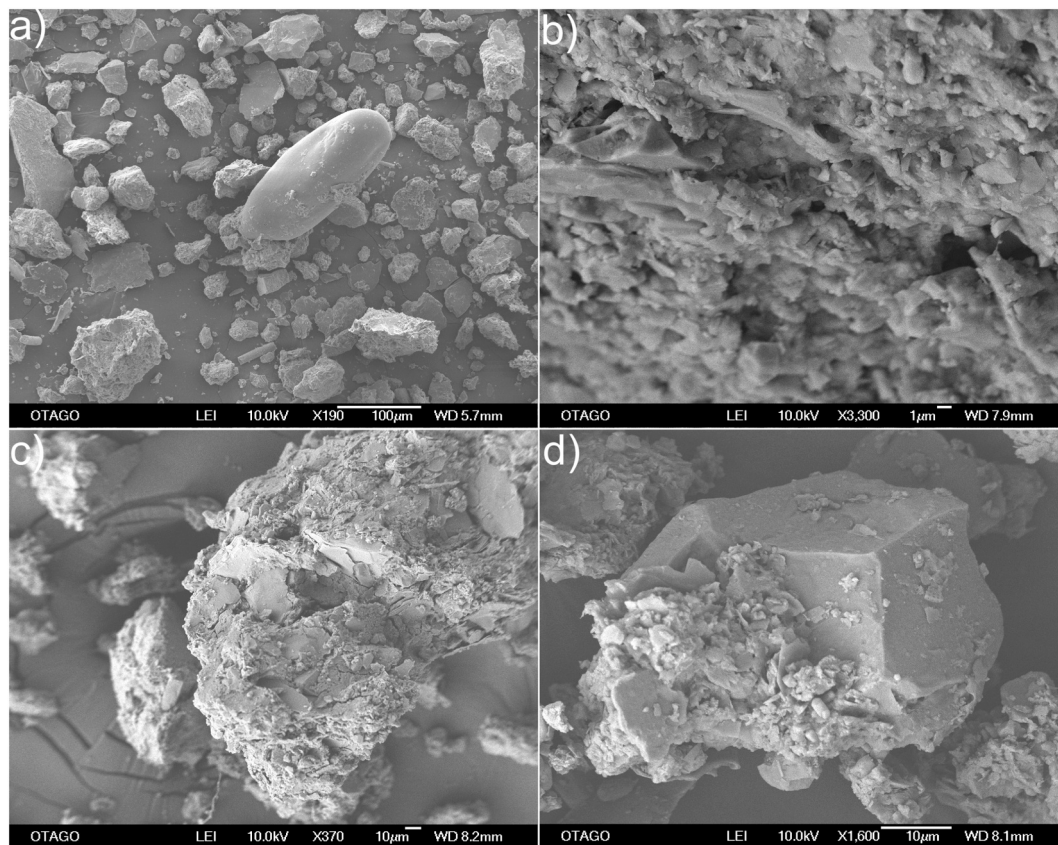


Fig. 11. Textural composition of entrained sediment on the platform at Mudstone Bay using SEM: a) smooth quartz grain amongst irregular blocky mudstone fragments caught in landward-facing sampler; b) rock fragments caught in landward-facing sampler; c) flocculated phyllosilicate minerals in seaward-facing sampler; d) smooth silicate mineral block likely plucked from platform surface in seaward-facing sampler.

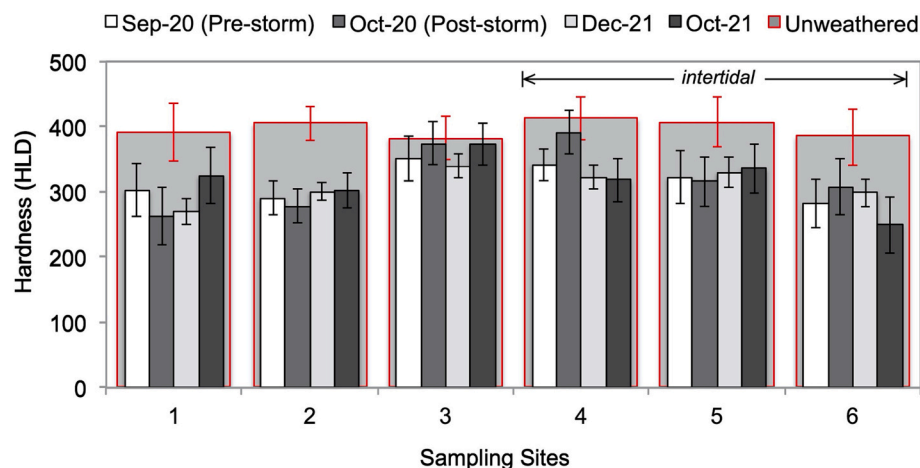


Fig. 12. Platform hardness measured using an Equotip durometer (HLD) as measured at six sampling stations at Mudstone Bay between September 2020 and December 2021.

5.3. Sediment production and mobility on supply-limited shore platforms

Wave hydrodynamics at the site of the sediment traps were low during the first part (tides 1–11) of the deployment ($<1 \text{ J m}^{-2}$), of which infragravity wave spectra contributed $\sim 37\%$ of the total energy. Under fair weather conditions little sediment movement was occurring or being collected in the traps. During the storm, however, total energy was 5 J m^{-2} and dominated by energy at infragravity frequencies (75 %). Under storm and subsequent post-storm conditions, infragravity energy

dominated the wave hydrodynamics, implying that long-waves (e.g., Ogawa et al., 2011; Poate et al., 2018) may be effective at sediment transport across shore platforms, as observed in highly dissipative beach environments (e.g., Beach and Sternberg, 1991; Hughes et al., 2014). The observations in this study are limited to only one sampling location on the shore platform and future work should assess whether sediment flux scales with infragravity energy by comparing changes in wave hydrodynamics across the shore platform under variable incident wave conditions.

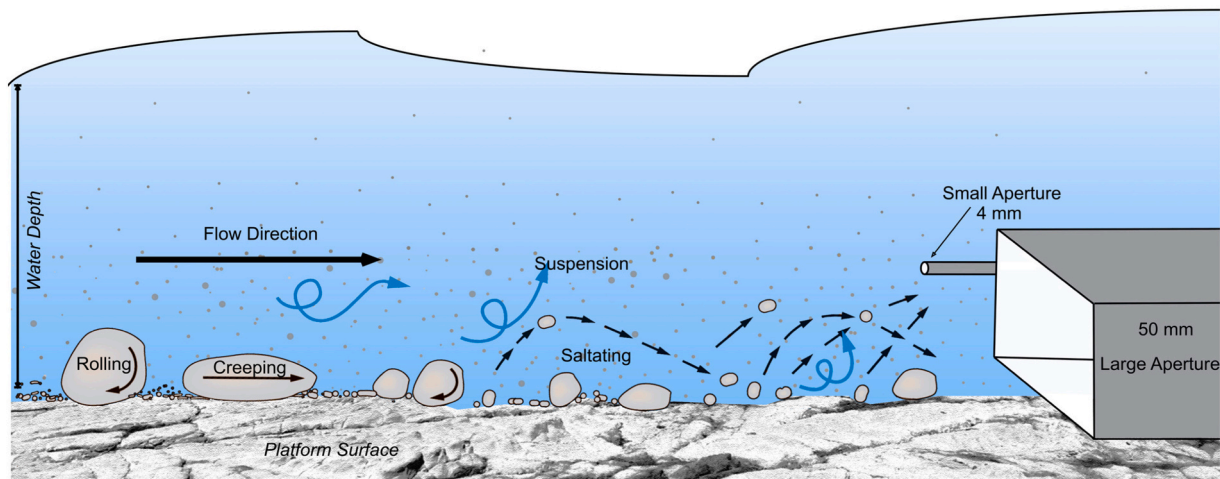


Fig. 13. Illustration showing the effect of the different sampler mouth sizes and positioning above the platform surface and possible sediment transport pathways.

During storm conditions saltating sediment was greatest in a seaward direction suggesting that on the shore platform there is sufficient backwash velocity to move material from the shore platform (i.e., unlimited transport capacity). There are differences in the potential flux directions between saltating and suspended load, with more suspended load being trapped landward. These data reveal a gap in the current understanding of sediment movement and flow dynamics on shore platforms, particularly as to why there might be a difference in sediment movement between the uprush and backwash. Observations on beaches have shown that backwash is mostly via tractive sediment movement through sheet flow drag (Horn and Mason, 1994; Hughes et al., 1997) because the main source of turbulence is from bed-shear, and there is insufficient upward momentum in the velocity profile of backwash to keep fine-grained sediment aloft in suspension. Recent observations on shore platforms have demonstrated complex wave interactions (Krier-Mariani et al., 2022) could influence the transport of sediment, but very little published research on sand to silt sized sediment transport on shore platforms is available. Further work is needed to quantify actual velocity of uprush and backwash on shore platforms, but it is possible that differences in sediment transport pathways occur between the uprush and backwash that may affect sediment entrainment (and thus trapped sediment).

The conceptual model of marine terrace development proposed by Dickson et al. (2022), informed in part by observations from Kaikōura, suggests that following co-seismic uplift sediment production occurs on the new supratidal surface from accelerated platform downwearing and from colluvial disaggregation, and may be nourished by episodic replenishment of onshore accumulation of storm deposits. Observations of the September–October 2020 storm at Kaikōura showed that wave conditions were insufficient to reach the back of the supratidal platform at Mudstone Bay with waves reaching an elevation of 1.2 m asl, and not to 1.6 m asl that would be needed to reach the supratidal deposits accumulated at the former (pre-uplift) cliff-toe. Based on the results of the sediment trapping experiments, it seems that mean annual storms are unlikely replenishing the supratidal deposits at Kaikōura, especially since there appears to be a seaward-dominance in fine-grained sediment transport at Mudstone Bay (i.e., sediment accumulation is away from the back of the platform). Rather, the build-up of sediment at the back of the supratidal platform at Kaikōura may be the result of in-situ accumulation of rock break-down or relict deposits associated with the 2016 uplift, rather than being post-uplift deposition associated with storm inundation. Given the small dataset presented in this pilot study, further research is required to confidently distinguish sediment provenance.

The potential geomorphic significance of these interpretations is relevant for paleo-earthquake investigations utilising chronological

information obtained from cover deposits (e.g., Litchfield et al., 2023). Evidence from the sediment traps implies that accumulation of deposits on top of incipient marine terraces (associated with uplifted shore platforms) could be syn-depositional features, rather than post-depositional storm deposits. The magnitude of uplift at Mudstone Bay appears to have been sufficient to move the former intertidal zone above the reach of most storm surge events. Calculation of inundation levels (Horton et al., 2022a) suggested that offshore waves between 4 and 6 m would need to coincide with high tide to provide sufficient surge to reach the back of the supratidal zone, and such wave conditions are possible but infrequent (i.e., annual exceedance probability <0.1). Thus, it is likely that only high magnitude and low frequency storms, or tsunami would likely have the potential to sweep material to the top of the incipient marine terrace.

6. Conclusions

Overall, this experiment has shown that:

- (i) Bi-directional TIMS can be used in sediment-poor shore platform environments for provenance studies;
- (ii) Both large and small aperture TIMS designs collected entrained sediments of a similar particle size and distribution;
- (iii) Large aperture TIMS are better suited to transport environments dominated by bedload movement, and can collect sufficient material to undertake sedimentary and geochemical analysis.

The deployment of sediment traps on the microtidal shore platform at Mudstone Bay has shown that under sub-annual storm conditions locally-sourced silt grade material is bi-directionally swept across the intertidal zone, with the greater flux heading seaward. In the context of Kaikōura the sediment trapping experiment has revealed that entrained sediments were aluminium silicates of autochthonous origin likely sourced from the platform and/or cliff-toe. Bedload movement was in a predominantly seaward direction so any material accumulation in the supratidal zone was unlikely emplaced by storms that were observed in this study. Rather, storms probably act to sweep free the platform surface from loose or disaggregated fine-granular material. Under storm conditions when sediment transport conditions were most favourable infragravity energy dominated the wave spectra at the TIMS location and may be effective in moving material in uprush and backwash, although it appears the suspended sediment concentration might be slightly greater in an onshore direction (landward) so that backwash is dominated by bedload movement. The future applications for this technique include resolving sediment budgets on intertidal shore

platforms and the mobility of back-beach material. Further work should also investigate sediment entrainment and flow velocities to advance our understanding of sediment transport in supply limited environments.

Funding

This research was funded by a Royal Society Te Apārangi Marsden Grant (UOO1828).

Declaration of competing interest

The authors declare that they have no known competing financial interests or personal relationships that could have appeared to influence the work reported in this paper.

Data availability

Data will be made available on request.

Acknowledgements

This research was funded by a Royal Society Te Apārangi Marsden grant (UOO1828). The authors are grateful to Takahanga Marae and acknowledge Kaikōura as Te Ahi kai koura a Tama ki te Rangi. Thank you to Te Runanga o Kaikōura of Takahanga Marae. Fieldwork was gratefully assisted by Jokotola Omidiji and Sarah Yeo. Laboratory analysis was supported by Gemma Kerr and Liz Girvan.

References

- Austin, M.J., Masselink, G., 2008. The effect of bedform dynamics on computing suspended sediment fluxes using optical backscatter sensors and current meters. *Coastal Engineering*. 55, 251–260.
- Ayeku, P.O., Ogundele, L.T., Ajibare, A.O., Aigbadon, G.O., 2021. Textural characteristics and geochemical composition of a tropical coastal marine sediment: a case study of transgressive mud beach, Bight of Benin, Nigeria. *Environmental Monitoring and Assessment*. 193, 729. <https://doi.org/10.1007/s10661-021-09533-w>.
- Bagnold, R.A., 1946. Motion of waves in shallow water: interaction between waves and sand bottoms. *Proc. R. Soc. London, Ser. A* 187, 1–18.
- Bagnold, R.A., 1966. An approach to the sediment transport problem from general physics. In: US Geological Survey Professional Paper, 422-I, Washington, D.C.
- Beach, R.A., Sternberg, R.W., 1991. Infragravity driven suspended sediment transport in the swash, inner and outer-surf zone. In: Kraus, N.C. (Ed.), *Coastal Sediments* (1991). American Society of Civil Engineering, pp. 114–128.
- Blanco-Chao, R., Pérez-Alberti, A., Costa-Casais, M., Valcárcel-Díaz, M., 2006. Abrasion processes in coarse-clastic beaches linked to rocky shore platforms. *Journal of Coastal Research*. SI 48, 21–28.
- Blanco-Chao, R., Pérez-Alberti, A., Trenhaile, A.S., Costa-Casais, M., Valcárcel-Díaz, M., 2007. Shore platform abrasion in a Para-periglacial environment, Galicia, northwestern Spain. *Geomorphology*. 83, 136–155.
- Bright, C.E., Mager, S.M., Horton, S.L., 2018. Predicting suspended sediment concentration from nephelometric turbidity in organic-rich waters. *River Res. Appl.* 34, 640–648.
- Butman, C.A., 1986. Sediment trap biases in turbulent flows: results from a laboratory flume study. *J. Mar. Res.* 44, 645–693.
- Chen, B., Chen, Z., Stephenson, W.J., Finlayson, B., 2011. Morphodynamics of a boulder beach, Putuo Island, SE China Coast: the role of storms and typhoon. *Marine Geology*. 283, 106–115.
- Coomes, M.A., Feal-Pérez, A., Naylor, L.A., Wilhelm, K., 2013. A non-destructive tool for detecting changes in the hardness of engineering materials: Application of the Equotip durometer in the coastal zone. *Eng. Geol.* 167, 14–19.
- Cullen, N.D., Bourke, M.C., 2018. Clast abrasion of a rock shore platform on the Atlantic coast of Ireland. *Earth Surf. Process. Landf.* 43, 2627–2641.
- Dickson, M.E., Omidiji, J., Litchfield, N.J., Norton, K.P., Matsumoto, H., Krier-Mariani, R. L., Horton, S.L., Acharya-Chowdhury, L., McLean, A.D., Hurst, M.D., Stephenson, W. J., 2022. Observations of the incipient and penultimate stages of Holocene marine terrace development. *Earth Surf. Process. Landf.* <https://doi.org/10.1002/esp.5440>.
- Dornbusch, U., Robinson, D.A., Williams, R.B.G., Moses, C.A., 2007. Chalk shore platform erosion in the vicinity of sea defense structures and the impact of construction methods. *Coast. Eng.* 54, 801–810.
- Duckmanton, N.M., 1974. The Shore Platforms of the Kaikōura Peninsula. Unpublished MA thesis, University of Canterbury, Christchurch, New Zealand, 136 pp.
- Duffy, B., 2020. A geometric model to estimate slip rates from terrace rotation above an offshore, listric thrust fault, Kaikōura, New Zealand. *Tectonophysics*. 786, 228460.
- Elliott, E.A., Monbureau, E., Walters, G.W., Elliott, M.A., McKee, B.A., Rodríguez, A.B., 2017. A novel method for sampling the suspended sediment load in the tidal environment using bi-directional time-integrated mass-flux sediment (TIMS) samplers. *Estuarine Coastal and Shelf Science*. 199, 14–24.
- Emmett, W.M., 1980. A field calibration of the sediment-trapping characteristics of the Helley-Smith bedload sampler. In: Geological Survey Professional Paper, 1139. <https://doi.org/10.3133/pp1139>.
- Etienne, S., Paris, R., 2010. Boulder accumulations related to storms on the south coast of the Reykjanes Peninsula (Iceland). *Geomorphology*. 114, 55–70.
- Feal-Pérez, A., Blanco-Chao, R., 2013. Characterization of abrasion surfaces in rock shore environments of NW Spain. *Geo-Mar. Lett.* 33, 173–181.
- Feal-Pérez, A., Blanco-Chao, R., Valcárcel-Díaz, M., 2009. Influencia de formas y procesos heredados en la evolución reciente y en los procesos morfodinámicos actuales en un sector de costa rocosa: Punta Gallín, costa cantábrica gallega. *Rev. Soc. Geol. Esp.* 22, 67–78.
- Ferguson, R.I., Church, M., 2004. A simple universal equation for grain settling velocity. *J. Sediment. Res.* 74, 933–937.
- Gee, G.W., Or, D. (2002). 2.4 Particle-size analysis. In: Dane, J.H., Topp, G.C. (Eds). *Methods in Soil Analysis*. Soil Science Society of America. doi: <https://doi.org/10.2136/sssabookser5.4.c12>.
- Gilbert, G.K., 1877. Report on the Geology of the Henry Mountains, Department of the Interior. U.S. Geographical and Geological Survey of Mountain Region, Washington, D.C., 170 pp.
- Gilbert, G.K., 1914. The Transportation of Debris by Running Water, U.S. In: Geological Survey Professional Paper. U.S. Geological Survey, Washington, D.C. 86, 263 Pp. U. S. Geological Survey, Washington, D.C.
- Hall, A.M., Hansom, J.D., Jarvis, J., 2008. Patterns and rates of erosion produced by high energy wave processes on hard rock headlands: the Grind of the Navir, Shetland, Scotland. *Marine Geology*. 248, 28–46.
- Horikawa, K., Sunamura, T., 1970. A study of erosion of coastal cliffs and submarine bedrocks. *Coastal Engineering in Japan*. 13, 127–139.
- Horn, D.P., Mason, T., 1994. Swash zone sediment transport modes. *Mar. Geol.* 120, 309–325.
- Horton, S.L., Stephenson, W.J., Dickson, M.E., 2022a. Supratidal inundation on an incipient marine terrace. *Geomorphology*. 417, 108443.
- Horton, S.L., Stephenson, W.J., Dickson, M.E., 2022b. Changes in shore platform wetting and drying cycles following the 2016 Kaikōura earthquake: implications for incipient marine terrace evolution. *Earth Surf. Process. Landf.* 47 (12), 2972–2988.
- Horton, S.L., Dickson, M.E., Stephenson, W.J., 2022c. The consequences of uplift on wave transformation across a shore platform, Kaikōura New Zealand. *Marine Geology*. 451, 106888.
- Howell, A., Clark, K., 2022. Late Holocene co-seismic uplift of the Kaikōura coast, New Zealand. *Geosphere* 18, 1104–1137. <https://doi.org/10.1130/GES02479.1>.
- Hughes, M.G., Masselink, G., Brander, R.W., 1997. Flow velocity and sediment transport in the swash zone of a steep beach. *Mar. Geol.* 138, 91–103.
- Hughes, M.G., Aagard, T., Baaldock, T.E., Power, H.E., 2014. Spectral signatures for swash on reflective, intermediate and dissipative beaches. *Mar. Geol.* 335, 88–97.
- Kennedy, D.M., 2015. Where is the seaward edge? A review and definition of shore platform morphology. *Earth Science Reviews*. 147, 99–108.
- Kennedy, D.M., Beban, J.G., 2005. Shore platform morphology on a rapidly uplifting coast, Wellington, New Zealand. *Earth Surface Processes and Landforms*. 30, 823–832.
- Kennedy, D.M., Dickson, M.E., 2006. Lithological control on the elevation of shore platforms in a microtidal setting. *Earth Surf. Process. Landf.* 31, 1575–1584.
- Kennedy, D.M., Milkins, J., 2015. The formation of beaches on shore platforms in microtidal environments. *Earth Surf. Process. Landf.* 40, 34–46.
- Kirk, R.M., 1971. Instruments for investigating shore and nearshore processes. *N. Z. J. Mar. Freshw. Res.* 5, 358–375.
- Kirk, R.M., 1975. Coastal changes at Kaikōura, 1942–74, determined from air photographs. *N. Z. J. Geol. Geophys.* 18 (6), 787–801.
- Kirk, R.M., 1977. Rates and forms of erosion on intertidal platforms at Kaikōura Peninsula, South Island, New Zealand. *New Zealand Journal of Geology and Geophysics*. 20, 571–613.
- Krier-Mariani, R.L., Stephenson, W.J., Wakes, S.J., Dickson, M.E., 2022. Perspectives on wave transformation over a near-horizontal shore platform: comparison of a two-dimensional and transect approach. *Geomorphology*. 405, 108200.
- Litchfield, N., Morgenstern, R., Clark, K., Howell, A., Grant, G., Turnbull, J., 2023. Holocene marine terraces as recorders of earthquake uplift: Insights from a rocky coast in southern Hawke's Bay, New Zealand. *Earth Surf. Process. Landf.* 48 (2), 452–474.
- Masselink, G., Puleo, J.A., 2006. Swash-zone morphodynamics. *Continental Shelf Research*. 26, 661–680.
- Masselink, G., Evans, D., Hughes, M.G., Russell, P., 2005. Suspended sediment transport in the swash zone of a dissipative beach. *Mar. Geol.* 216, 169–189.
- McDonald, D.M., Lamoureux, S.F., Warburton, J., 2010. Assessment of a time-integrated fluvial suspended sediment sampler in a high arctic setting. *Geogr. Ann. Ser. Aephys. Geogr.* 92A, 225–235.
- McFadden, B.G., 1987. Beach ridges, breakers and bones: late Holocene geology and archaeology of the Fyffe site, S49/46, Kaikōura Peninsula, New Zealand. *Journal of the Royal Society of New Zealand*. 17, 381–394.
- McKenna, J., Jackson, D.W.T., Cooper, J.A.C., 2011. In situ exhumation from bedrock of large rounded boulders at the Giant's Causeway, Northern Ireland: an alternative genesis for large shore boulders (mega-clasts). *Mar. Geol.* 283, 25–35.
- Minor, E.C., Swenson, M.M., Mattson, B.M., Oyler, A.R., 2014. Structural characterisation of dissolved organic matter: a review of current techniques for isolation and analysis. *Environ. Sci.: Processes Impacts* 16, 2064–2079.

- Morris, J.C., 1987. The stratigraphy of the Amuri limestone group, East Marlborough, New Zealand. PhD Thesis. University of Canterbury, p. 439.
- Moses, C., Robinson, D., 2011. Chalk coast dynamics: implications for understanding rock coast evolution. *Earth Sci. Rev.* 109, 63–73.
- Moses, C.A., 2014. The rock coast of the British Isles: shore platforms. In: Kennedy, D.M., Stephenson, W.J., Naylor, L.A. (eds). *Rock Coast Geomorphology: a Global Synthesis*. Geological Society, London. Memoirs. 40, 39–56.
- Naylor, L.A., Coombes, M.A., Viles, H.A., 2012. Reconceptualising the role of organisms in the erosion of rock coasts: A new model. *Geomorphology* 157–158, 17–30.
- Naylor, L.A., Stephenson, W.J., Smith, H.C.M., Way, O., Mendelssohn, J., Cowley, A., 2016. Geomorphological control on boulder transport and coastal erosion before, during and after an extreme extra-tropical cyclone. *Earth Surf. Process. Landf.* 41, 685–700.
- Nicol, A., Begg, J., Saltogianni, V., Mouslopoulou, V., Oncken, O., Howell, A., 2022. Uplift and fault slip during the 2016 Kaikōura earthquake and late Quaternary, Kaikōura Peninsula, New Zealand. *New Zealand Journal of Geology and Geophysics*. 66 (2), 263–278.
- Nott, J., 2003. Waves, coastal boulder deposits, and the importance of the pre-transport setting. *Earth Planet. Sci. Lett.* 210, 269–276.
- Ogawa, H., Dickson, M.E., Kench, P.S., 2011. Wave transformation on a sub-horizontal shore platform, Tatapouri, North Island, New Zealand. *Continental Shelf Research*. 31, 1409–1419. <https://doi.org/10.1016/j.csr.2011.05.006>.
- Omidiji, J., Stephenson, W., Dickson, M., Norton, K., 2022. Tectonics and shore platform development: rates and patterns of erosion on recently uplifted mudstone and limestone rocks at Kaikōura Peninsula, New Zealand. *Marine Geology*. 451, 106887.
- Ota, Y., Pillans, B., Berryman, K., Beu, R., Fujimori, T., Miyauchi, T., Berger, G., Beu, A. G., Climo, F.M., 1996. Pleistocene coastal terraces of Kaikōura Peninsula and the Marlborough coast, South Island, New Zealand. *New Zealand Journal of Geology and Geophysics*. 39, 51–73.
- Paris, R., Naylor, L.A., Stephenson, W.J., 2011. Boulders as a signature of storms on rock coasts. *Mar. Geol.* 283, 1–11.
- Pérez-Alberti, A., Trenhaile, A.S., Pires, A., López-Bedoya, J., Chaminé, H.I., Gomes, A., 2012. The effect of boulders on shore platform development and morphology in Galicia, north West Spain. *Cont. Shelf Res.* 48, 122–137.
- Perks, M.T., Warburton, J., Bracken, L., 2013. Critical assessment and validation of a time-integrating fluvial suspended sediment sampler. *Hydrol. Process.* 28, 4795–4807.
- Phillips, J.M., Russell, M.A., Walling, D.E., 2000. Time-integrated sampling of fluvial suspended sediment, a simple methodology for small catchments. *Hydrol. Process.* 14, 2589–2602.
- Poate, T., Masselink, G., Austin, M.J., Dickson, M., McCall, R., 2018. The Role of Bed Roughness in Wave Transformation across Sloping Rock Shore Platforms. *J. Geophys. Res. Earth Surf.* 123, 97–123. <https://doi.org/10.1002/2017JF004277>.
- Porter, N.J., Trenhaile, A.S., Prestanski, K.J., Kanyaya, J.I., 2010. Shore platform downwearing in eastern Canada: the mega-tidal Bay of Fundy. *Geomorphology*. 118, 1–12.
- Power, W., Clark, K., King, D.N., Borrero, J., Howarth, J., Lane, E.M., Goring, D., Goff, J., Chagué-Goff, C., Williams, J., Reid, C., Whittaker, C., Mueller, C., Williams, S., Hughes, M.W., Hoyle, J., Bind, J., Strong, D., Litchfield, N., Benson, A., 2017. Tsunami runup and tide-gauge observations from the 14 November 2016 M7.8 Kaikōura earthquake, New Zealand. *Pure Appl. Geophys.* 174, 2457–2473.
- Rattenbury, M.S., Townsend, D.B., Johnston, M.R., 2006 (compilers). *Geology of the Kaikōura Area*. Institute of Geological & Nuclear Sciences 1:250 000 geological map 13. 1 sheet + 70p. Lower Hutt, New Zealand, GNS Science.
- Robinson, L.A., 1977. Marine erosive processes at the cliff foot. *Mar. Geol.* 23, 257–271.
- Schiel, D.R., Wood, S.A., Dunmore, R.A., Taylor, D.I., 2006. Sediment on rocky intertidal reefs: effects on early post-settlement stages of habit-forming seaweeds. *J. Exp. Mar. Biol. Ecol.* 331, 158–172.
- Shetty, A., Jayappa, K.S., Deepak, P.R., Ratheesh, R., 2022. Nearshore suspended sediment concentration and transport pattern along the southern Karnataka coast India. *Journal of Sedimentary Environments*. 7, 95–110.
- Stephenson, W.J., Kirk, R.M., 2000. Development of shore platforms on Kaikōura Peninsula, south Island, New Zealand. II: the role of subaerial weathering. *Geomorphology*. 32, 43–56.
- Stephenson, W.J., Dickson, M.E., Denys, P.H., 2017. New insights on the relative contributions of coastal processes and tectonics to shore platforms development following the Kaikōura earthquake. *Earth Surf. Process. Landf.* 42, 2214–2220. <https://doi.org/10.1002/esp.4176>.
- Trenhaile, A.S., 2004. Modeling the accumulation and dynamics of beaches on shore platforms. *Mar. Geol.* 206, 55–72.
- Trenhaile, A.S., 2005. Modelling the effect of waves, weathering and beach development on shore platform development. *Earth Surf. Process. Landf.* 30, 613–634.
- Trenhaile, A.S., 2016. Rocky coasts — their role as depositional environments. *Earth-Science Reviews*. 159, 1–13.
- Viles, H., Goudie, A., Grab, S., Lalley, J., 2011. The use of the Schmidt Hammer and Equotip for rock hardness assessment in geomorphology and heritage science: a comparative analysis. *Earth Surf. Process. Landf.* 36, 320–333.
- Wainwright, J., Parsons, A.J., Cooper, J.R., Gao, P., Gillies, J.A., Mao, L., Orford, J.D., Knight, P.G., 2015. The concept of transport capacity in geomorphology. *Rev. Geophys.* 53, 1155–1202.
- Wallace, L.M., Barnes, P., Beavan, J., Van Dissen, R., Litchfield, N., Mountjoy, J., Langridge, R., Lamarche, G., Pondard, N., 2012. The kinematics of a transition from subduction to strike-slip: an example from the Central New Zealand plate boundary. *Journal of Geophysical Research* 117. <https://doi.org/10.1029/2011JB008640>. Bo2405.
- White, J., 1990. The use of sediment traps in high-energy environments. *Mar. Geophys. Res.* 12, 145–152.